











Structural and transport properties of La tungstate and its composite with nickel (II) and copper (II) oxides

Nikita Ereemeev ^{a*} , Yulia Bepalko ^a , Ekaterina Sadovskaya ^a, Tamara Krieger ^a ,
Svetlana Cherepanova ^a , Evgeny Suprun ^a , Arcady Ishchenko ^a , Mikhail
Mikhailenko ^b , Mikhail Korobeynikov ^c, Vladislav Sadykov ^a 

^a Federal Research Center Boreskov Institute of Catalysis SB RAS, Novosibirsk
630090, Russia

^b Institute of Solid State Chemistry and Mechanochemistry SB RAS, Novosibirsk
630128, Russia

^c Budker Institute of Nuclear Physics SB RAS, Novosibirsk 630090, Russia

* (E-mail: yeremeev21@catalysis.ru)

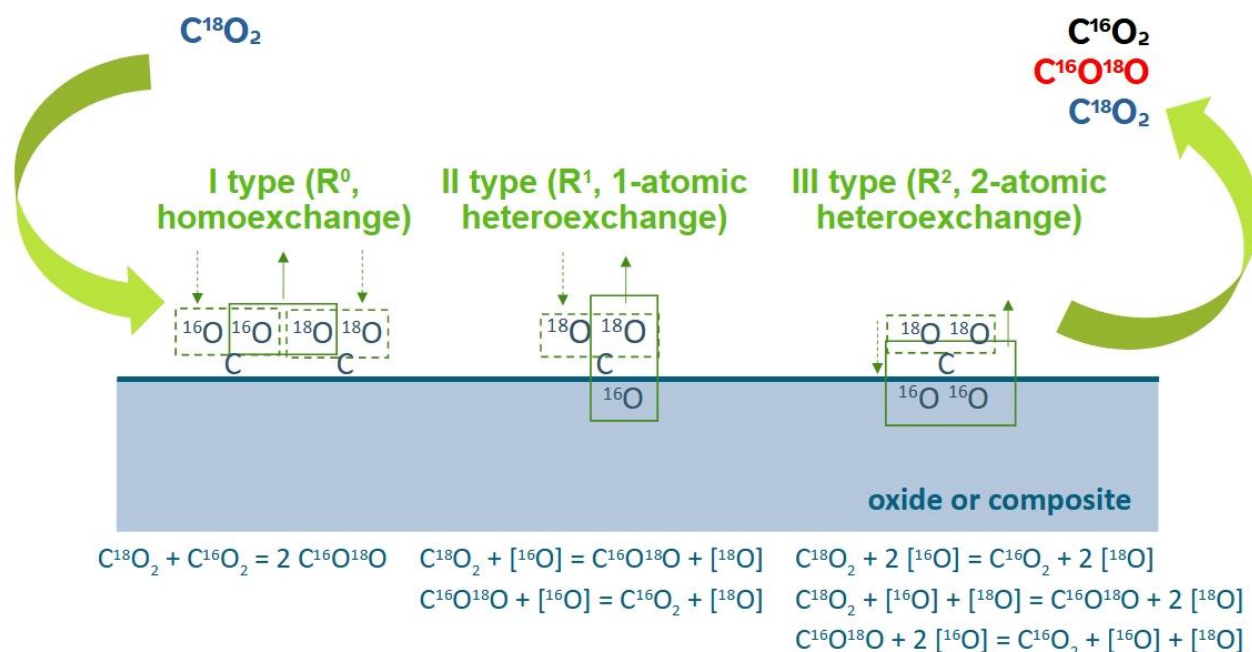


Figure S1 Principle of isotope exchange of oxygen with C^{18}O_2 and three types of exchange mechanisms according to the Muzykantov's classification [S1].

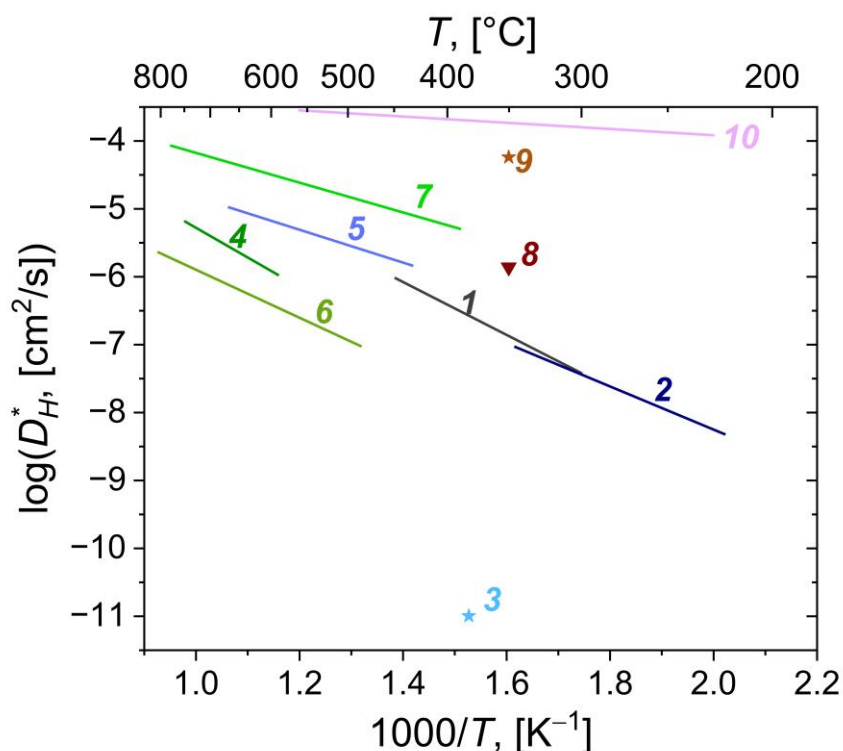
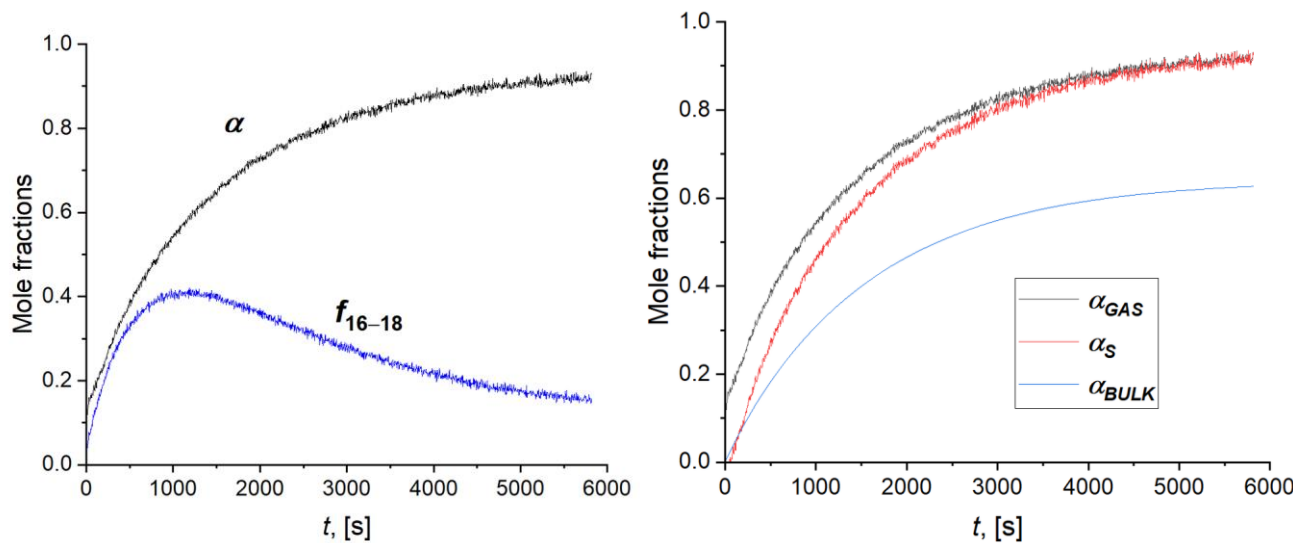


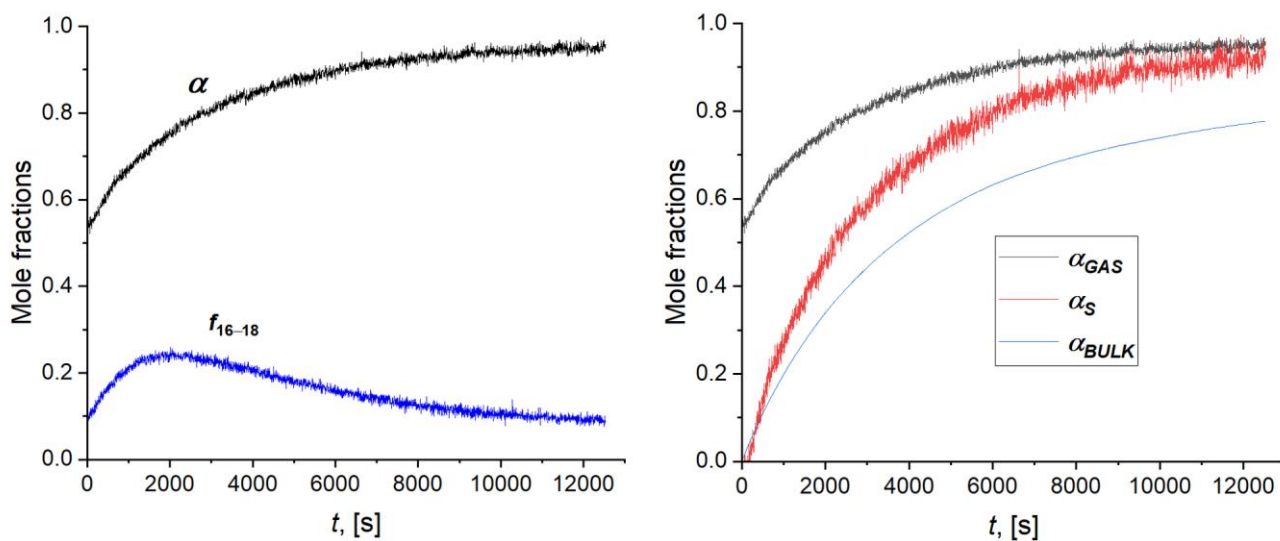
Figure S2 Arrhenius plots for hydrogen tracer diffusion coefficient values for various proton-conducting materials: 1 - $\text{La}_{27.15}\text{W}_{4.85}\text{O}_{55-\delta}$ [S2]; 2 - $\text{La}_{27.15}\text{W}_{4.85}\text{O}_{55-\delta}$ [S3]; 3 - $\text{Nd}_{5.5}\text{WO}_{11.25-\delta}$ [S4]; 4 - $\text{Sr}_{1.95}\text{Fe}_{1.5}\text{Mo}_{0.5}\text{O}_{6-\delta}$ [S5,S6]; 5 - $\text{BaCe}_{0.9}\text{Y}_{0.1}\text{O}_{3-\delta}$ [S5,S7], 6 - $\text{La}_{0.91}\text{Sr}_{0.09}\text{ScO}_{3-\delta}$ [S8]; 7 - Ni [S5,S9]; 8 - $\text{Cu}_{0.447}\text{Pd}_{0.553}$ [S10]; 9 - $\text{Cu}_{0.554}\text{Pd}_{0.446}$ [S10]; 10 - V [S11].



(a)

(b)

Figure S3 The experimental time dependencies of ^{18}O and $^{16}\text{O}^{18}\text{O}$ fractions in the gas phase (a), and ^{18}O fraction in the gas phase, on the sample surface and in the sample bulk (b) for LWO sample according to IIE with $^{18}\text{O}_2$ at 800 °C.



(a)

(b)

Figure S4 The experimental time dependencies of ^{18}O and $^{16}\text{O}^{18}\text{O}$ fractions in the gas phase (a), and ^{18}O fraction in the gas phase, on the sample surface and in the sample bulk (b) for LWORT sample according to IIE with $^{18}\text{O}_2$ at 800 °C.

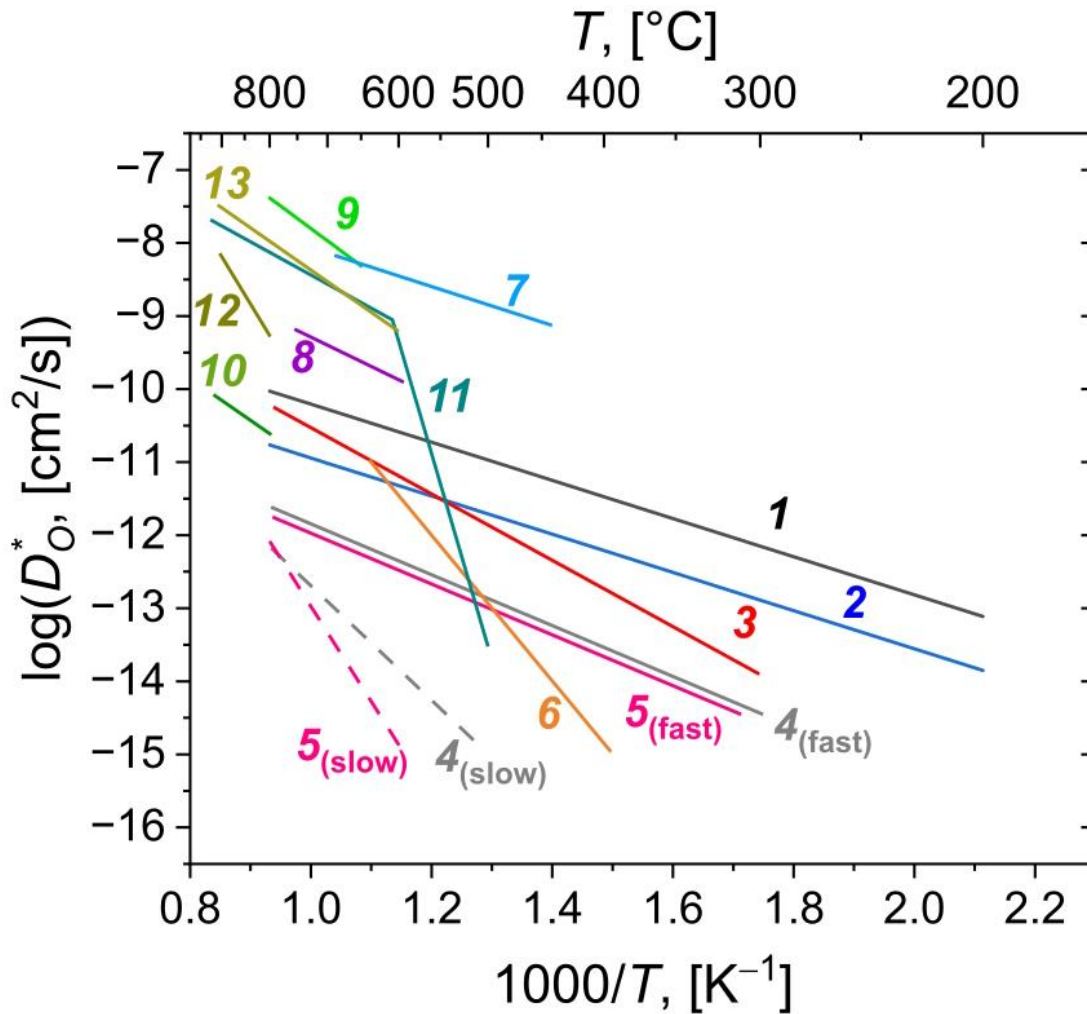


Figure S5 Arrhenius plots for oxygen tracer diffusion coefficient values for various proton-conducting materials: 1 - $\text{La}_{27}\text{W}_5\text{O}_{55.5-\delta}$ (LWO, this work); 2 - $\text{La}_{27}\text{W}_5\text{O}_{55.5-\delta}$ (LWO_{RT}, this work); 3 - $\text{Er}_{5.5}\text{MoO}_{11.25-\delta}$ [S12]; 4 - $\text{La}_{0.99}\text{Ca}_{0.01}\text{NbO}_4$ [S13]; 5 - $\text{La}_{0.99}\text{Ca}_{0.01}\text{NbO}_4\text{-LaNb}_3\text{O}_9$ [S13]; 6 - $\text{Sm}_{1.9}\text{Ca}_{0.1}\text{ScTaO}_{7-\delta}$ [S14]; 7 - $\text{La}_{9.83}\text{Si}_5\text{Al}_{0.75}\text{Fe}_{0.25}\text{O}_{26.5}$ [S15]; 8 - $\text{Ca}_3\text{Co}_4\text{O}_{9\pm\delta}$ [S16]; 9 - $\text{Sr}_{1.95}\text{Fe}_{1.4}\text{Ni}_{0.1}\text{Mo}_{0.5}\text{O}_{6-\delta}$ [S17]; 10 - $\text{BaZr}_{0.80}\text{Y}_{0.20}\text{O}_{3-\delta}$ [S18]; 11 - $\text{BaCe}_{0.9}\text{La}_{0.1}\text{O}_{3-\delta}$ [S19]; 12 - $\text{LaScO}_{3-\delta}$ [S20]; 13 - $\text{La}_{0.91}\text{Sr}_{0.09}\text{ScO}_{3-\delta}$ [S20].



Supplementary references

- S1. Muzykantov VS, Popovski VV, Boreskov GK. Kinetika izotopnogo obmena v sisteme molekulyarnyi kislorod - tvyodyi okisel [Kinetics of isotope exchange in molecular oxygen - solid oxide system]. Kinet Katal. 1964;5(4):624-9. Russian.
- S2. Hancke R, Li Z, Haugrud R. Thermogravimetric relaxation study of the proton conductor lanthanum tungstate, $\text{La}_{28-x}\text{W}_{4+x}\text{O}_{54+\delta}\text{V}_{2-\delta}$, $x = 0.85$. Int J Hydrog Energy. 2012;37(9):8043-50. doi:[10.1016/j.ijhydene.2011.11.050](https://doi.org/10.1016/j.ijhydene.2011.11.050)
- S3. Hancke R, Fearn S, Kilner JA, Haugrud R. Determination of proton- and oxide ion tracer diffusion in lanthanum tungstate (La/W = 5.6) by means of ToF-SIMS. Phys Chem Chem Phys. 2012;14(40):13971-8. doi:[10.1039/c2cp42278f](https://doi.org/10.1039/c2cp42278f)
- S4. Sadykov VA, Bepalko YuN, Pavlova SN, Skriabin PI, Krasnov AV, Ereemeev NF, Krieger TA, Sadovskaya EM, Belyaev VD, Vinokurov ZS. Protonic mobility of neodymium tungstate. J Electrochem En Conv Stor. 2017;14(4):044501. doi:[10.1115/1.4037957](https://doi.org/10.1115/1.4037957)
- S5. Osinkin DA. Electrochemical behaviour of redox-robust electrode in contact with protonic electrolyte: Case of double-layered $\text{Sr}_2\text{Fe}_{1.5}\text{Mo}_{0.5}\text{O}_{6-\delta}$ - $\text{Ce}_{0.8}\text{Sm}_{0.2}\text{O}_{2-\delta}$ composite. Int J Hydrog Energy. 2024;77:1066-73. doi:[10.1016/j.ijhydene.2024.06.266](https://doi.org/10.1016/j.ijhydene.2024.06.266)
- S6. Ren R, Sun J, Wang G, Xu C, Qiao J, Sun W, Wang Z, Sun K. Rational design of $\text{Sr}_2\text{Fe}_{1.5}\text{Mo}_{0.4}\text{Y}_{0.1}\text{O}_{6-\delta}$ oxygen electrode with triple conduction for hydrogen production in protonic ceramic electrolysis cell. Sep Purif Technol. 2022;299:121780. doi:[10.1016/j.seppur.2022.121780](https://doi.org/10.1016/j.seppur.2022.121780)
- S7. Kreuer KD. Aspects of the formation and mobility of protonic charge carriers and the stability of perovskite-type oxides. Solid State Ionics. 1999;125 (1-4):285-302. doi:[10.1016/S0167-2738\(99\)00188-5](https://doi.org/10.1016/S0167-2738(99)00188-5)
- S8. Farlenkov AS, Vlasov MI, Porotnikova NM, Bobrikov IA, Khodimchuk AV, Ananyev MV. Hydrogen diffusivity in the Sr-doped LaScO_3 proton-conducting oxides. Int J Hydrog Energy. 2020;45(43):23455-6810. doi:[10.1016/j.ijhydene.2020.06.148](https://doi.org/10.1016/j.ijhydene.2020.06.148)
- S9. Edwards AG. Measurement of the diffusion rate of hydrogen in nickel. Br J Appl Phys. 1958;8(10):406-10. doi:[10.1088/0508-3443/8/10/306](https://doi.org/10.1088/0508-3443/8/10/306)
- S10. Piper J. Diffusion of hydrogen in copper-palladium alloys. J Appl Phys. 1966;37(2):715-21. doi:[10.1063/1.1708243](https://doi.org/10.1063/1.1708243)
- S11. Huang F, Li X, Shan X, Guo J, Gallucci F, Annaland MVS, Liu D. Hydrogen transport through the V-Cr-Al Alloys: Hydrogen solution, permeation and thermal-stability. Sep Purif Technol 2020;240:116654. doi:[10.1016/j.seppur.2020.116654](https://doi.org/10.1016/j.seppur.2020.116654)
- S12. Shlyakhtina AV, Lyskov NV, Šalkus T, Kežionis A, Patrakeev MV, Leonidov IA, Shcherbakova LG, Chernyak SA, Shefer KI, Sadovskaya EM, Ereemeev NF, Sadykov VA. Conductivity and oxygen diffusion in bixbyites and fluorites $\text{Ln}_{6-x}\text{MoO}_{12-\delta}$ (Ln = Er, Tm; $x = 0, 0.5$). Int J Hydrog Energy. 2021;46(32):16965-76. doi:[10.1016/j.ijhydene.2021.02.029](https://doi.org/10.1016/j.ijhydene.2021.02.029)
- S13. Sadykov VA, Bepalko YuN, Krasnov AV, Skriabin PI, Lukashevich AI, Fedorova YuE, Sadovskaya EM, Ereemeev NF, Krieger TA, Ishchenko AV, Belyaev VD, Uvarov NF, Ulihin AS, Skovorodin IN. Novel proton-conducting nanocomposites for hydrogen separation membranes. Solid State Ionics. 2018;322:69-78. doi:[10.1016/j.ssi.2018.05.003](https://doi.org/10.1016/j.ssi.2018.05.003)
- S14. Shlyakhtina AV, Pigalskiy KS, Belov DA, Lyskov NV, Kharitonova EP, Kolbanev IV, Borunova AB, Karyagina OK, Sadovskaya EM, Sadykov VA, Ereemeev NF. Proton and oxygen ion conductivity in the pyrochlore/fluorite family of $\text{Ln}_{2-x}\text{Ca}_x\text{ScMO}_{7-\delta}$ (Ln = La, Sm, Ho, Yb; M = Nb, Ta; $x = 0, 0.05, 0.1$) niobates and tantalates. Dalton Trans. 2018;47(7):2376-92. doi:[10.1039/c7dt03912c](https://doi.org/10.1039/c7dt03912c)
- S15. Sadykov VA, Sadovskaya EM, Ereemeev NF, Skriabin PI, Krasnov AV, Bepalko YuN, Pavlova SN, Fedorova YuE, Pikalova EYu, Shlyakhtina AV. Oxygen mobility in the materials for solid oxide fuel cells and catalytic membranes (Review). Russ J Electrochem. 2019;55(8):701-18. doi:[10.1134/S1023193519080147](https://doi.org/10.1134/S1023193519080147)
- S16. Thoréton V, Hu Y, Pirovano C, Capoen E, Nuns N, Mamede AS, Dezanneau G, Yoo CY, Bouwmeester HJM, Vannier RN. Oxygen transport kinetics of the misfit layered oxide $\text{Ca}_3\text{Co}_4\text{O}_{9+\delta}$. J Mater Chem A. 2014;2(46):19717-25. doi:[10.1039/C4TA02198C](https://doi.org/10.1039/C4TA02198C)



- S17. Porotnikova NM, Khodimchuk AV, Zakharov DM, Bogdanovich NM, Osinkin DA. Enhancement of surface exchange and oxygen diffusion of $\text{Sr}_{1.95}\text{Fe}_{1.4}\text{Ni}_{0.1}\text{Mo}_{0.5}\text{O}_{6-\delta}$ oxide determined by two independent isotope exchange methods. *Appl Surf Sci.* 2023;613:156015. doi:[10.1016/j.apsusc.2022.156015](https://doi.org/10.1016/j.apsusc.2022.156015)
- S18. Farlenkov AS, Ananyev MV, Eremin VA, Porotnikova NM, Kurumchin EK, Melekh B-T. Oxygen isotope exchange in doped calcium and barium zirconates. *Solid State Ionics.* 2016;290:108-15. doi:[10.1016/j.ssi.2016.04.015](https://doi.org/10.1016/j.ssi.2016.04.015)
- S19. De Souza RA, Kilner JA, Jeynes C. The application of secondary ion mass spectrometry (SIMS) to the study of high temperature proton conductors (HTPC). *Solid State Ionics.* 1997;97(1-4):409-19. doi:[10.1016/S0167-2738\(97\)00038-6](https://doi.org/10.1016/S0167-2738(97)00038-6)
- S20. Farlenkov AS, Khodimchuk AV, Shevyrev NA, Stroeva AY, Fetisov AV, Ananyev MV. Oxygen isotope exchange in proton-conducting oxides based on lanthanum scandates. *Int J Hydrog Energy.* 2019;44(48):26577-88. doi:[10.1016/j.ijhydene.2019.08.088](https://doi.org/10.1016/j.ijhydene.2019.08.088)